Supplementary Material

for

A Magnetic Core-shell-structured FeO_x/CN Catalyst Mediated Peroxymonosulfate Activation for Degradation of 2,4-Dichlorophenol via Nonradical Pathway

Kaijie Xu [a], Kangping Cui [a*], Chenxuan Li [a], Minshu Cui [a], Rohan Weerasooriya [b, c], Xiaoyang Li [d], Zhaogang Ding [a, b], Xing Chen [a, b*]

[a] Key Laboratory of Nanominerals and Pollution Control of Higher Education Institutes, School of Resources and Environmental Engineering, Hefei University of Technology, Hefei, 230009, China

[b] Key Lab of Aerospace Structural Parts Forming Technology and Equipment of Anhui Province, Institute of Industry and Equipment Technology, Hefei University of Technology, Hefei, 230009, China

[c] National Centre for Water Quality Research, National Institute of Fundamental Studies Hantana, Kandy, Sri Lanka

[d] State Key Laboratory of Pollution Control and Resource Reuse, School of the Environment, Nanjing University, Nanjing, 210023, China

* Corresponding author.

Text captions

Table captions

Figure captions

Text S1. Chemicals

All the chemicals were used directly without further purification. 2,4-dichlorophenol (2,4-DCP, 99%), sodium thiosulfate ($Na_2S_2O_3$), ferric nitrate (Fe $(NO_3)_3 \cdot 9H_2O$), tert-butyl alcohol (TBA, 99.9%), acetonitrile, and methanol (MeOH) of HPLC grade were purchased from Sinopharm Chemical Reagent Co., Ltd. 5,5-di-methyl-1-pyrroline-N-oxide (DMPO, 99%) and 2,2,6,6-Tetramethyl-4-piperidinol (TEMP, 99%) for EPR-spectroscopy were purchased from Jiuding Chemistry. Triethylenediamine hexahydrate (DABCO), Benzoic acid (BA), p-hydroxybenzoic acid (HBA), and p-benzoquinone (BQ) were all purchased from Aladdin Chemistry Co., Ltd (Shanghai, China).

Text S2. Details for the probe experiment.

In this study, the quantification of free radicals during the reaction was obtained indirectly by HPLC. First, excess HBA reacted with the $SO_4^{\bullet-}$ in the solution to form hydroquinone, which was unstable, and then the hydroquinone further converted into stable BQ. By measuring the amount of BQ produced, the concentration of $SO_4^{\bullet-}$ could be obtained indirectly. For ·OH, with excessive BA, ·OH was quickly consumed, and HBA was accumulated. Based on the measurement results of HBA, the amount of ·OH produced was estimated [1, 2]. The detailed test conditions are shown in Table S1.

Table S1. HPLC analysis conditions for different organics.

Analyte	Mobile phase	Flow rate ml/min	UV radiation nm
2,4-DCP	2:8 (v/v) water: methanol	1.00	282
HBA	6:4 (v/v) 0.1 % H_3PO_4: acetonitrile	1.00	265
BQ	1:1 (v/v) water: acetonitrile	0.75	246

Table S2. Degradation intermediate of 2,4-DCP detected by GC-MS.

Product	$[M+H]^+$ (m/z)	Molecular formula	Structural formula
A(2,4-DCP)	162	$C_6H_4Cl_2O$	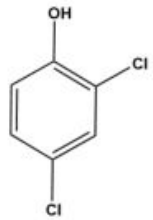
B	144	$C_6H_5ClO_2$	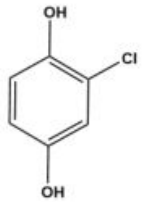
E	128	C_6H_5ClO	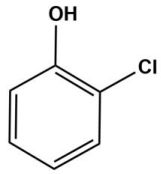
F	178	$C_6H_4Cl_2O_2$	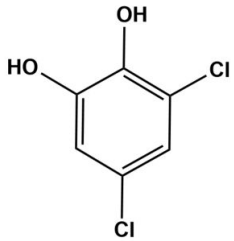
K	94	C_6H_6O	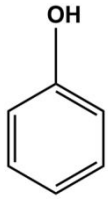

O	100	$C_6H_{12}O$	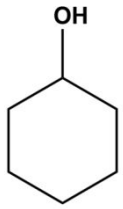
Q	74	$C_3H_6O_2$	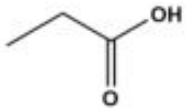
R	60	$C_2H_4O_2$	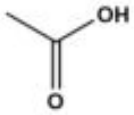
S	90	$C_2H_2O_4$	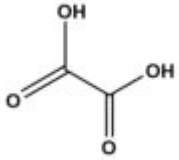

Table S3. Iron contents of Fe-X/CN.

	Fe-1/CN	Fe-2/CN	Fe-3/CN	Fe-4/CN	Fe-5/CN
Fe content wt %	24.03	46.35	59.49	68.65	75.86

Table S4. Comparison of the catalytic activities of Fe-3/CN with the transition metal catalysts in the literature.

Catalyst	Catalyst dose ($g\ L^{-1}$)	PMS[a] / H_2O_2[b] ($g\ L^{-1}$)	Contaminant	[Contaminant] ($mg\ L^{-1}$)	pH	T (□)	TOF	Mineralization (%)	Ref.
Co^{2+}@PMAP	0.4	1.8 [a]	Phenol	10	7	45	0.185	42	1
DPA-hematite	0.5	2.0 [a]	BPA	15	7	RT	0.078	22	2
Fe-ZSM-5	1.5	0.6 [b]	Phenol	10	3.5	70			3
Fe/AC	0.5	0.5 [b]	Phenol	6.5	3	50		85	4
Fe-3/CN	0.5	0.15 [a]	Chlorophenol	5	6.5	RT	0.33	88	This work

RT= Room Temperature

Ref.

1. RSC Advances 2015, 5 (10), 7628-7636.

2. J Mater Chem A 2014, 2 (38), 15836-15845.

3. Applied Catalysis B: Environmental 1996, 10 (4), L229-L235.

4. Applied Catalysis B: Environmental 2006, 65 (3), 261-268.

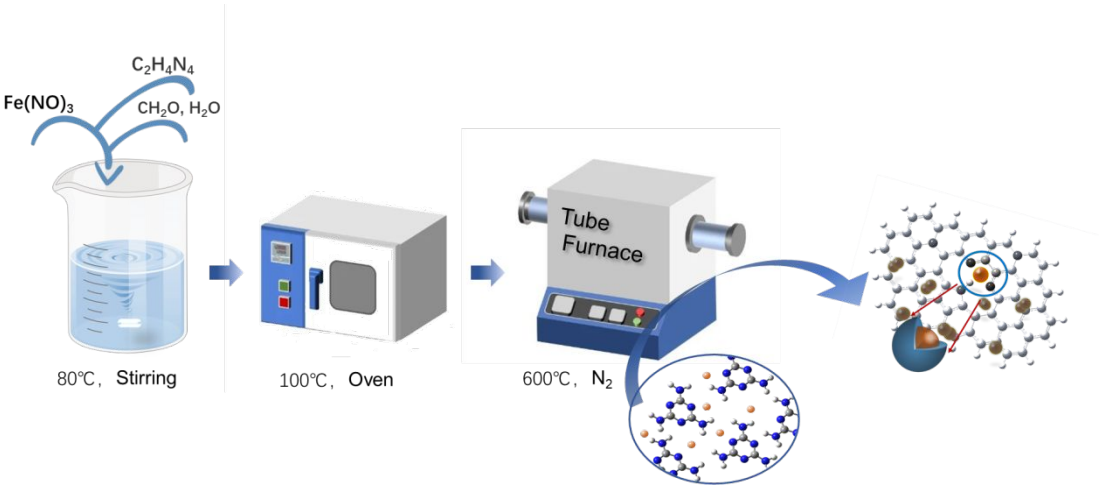

Fig. S1. Schematic illustration of the synthesis FeO_x/CN catalyst.

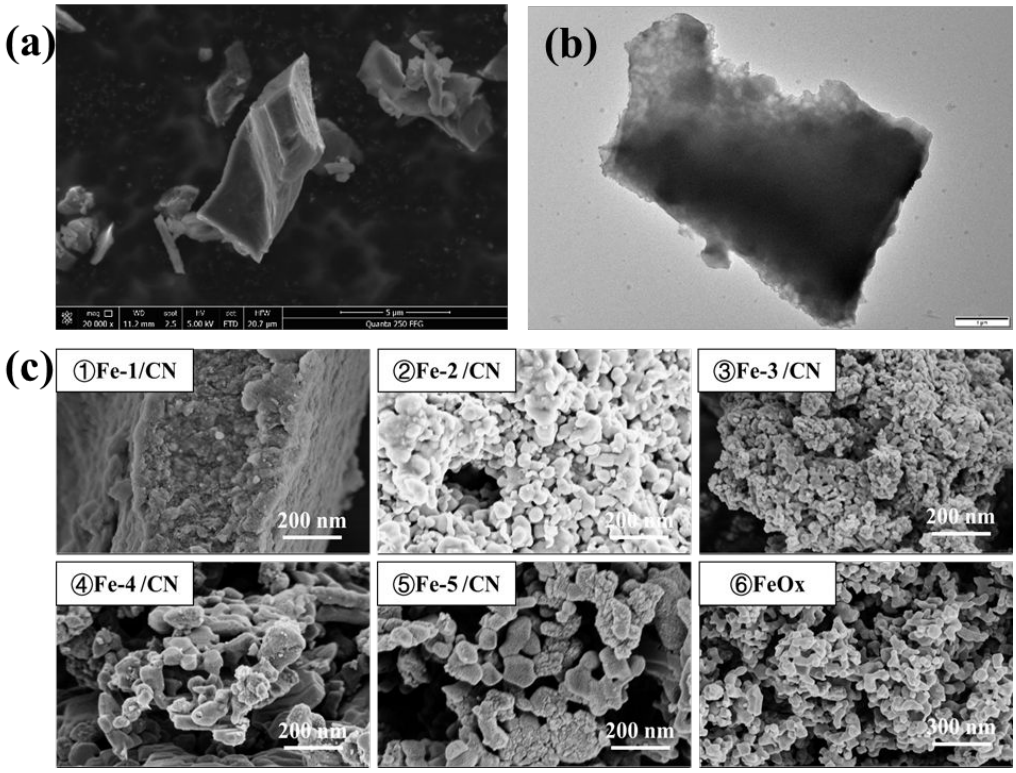

Fig. S2. SEM imagine(a) and TEM imagine(b) of CN; SEM images of Fe-X/CN (X=1, 2, 3, 4, and 5) and Pure FeO_x (c).

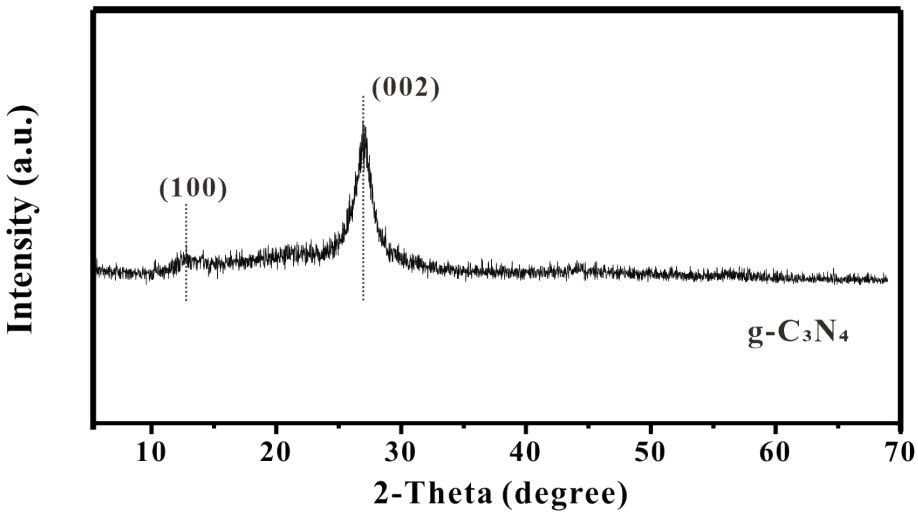

Fig. S3. XRD spectrum of g-C_3N_4.

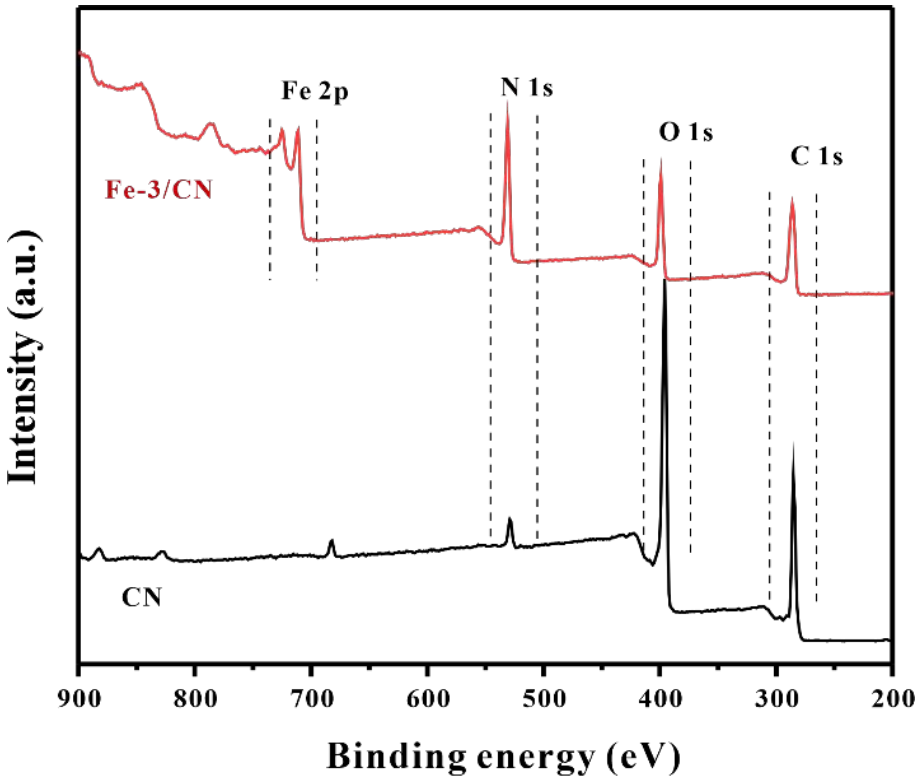

Fig. S4. XPS survey spectra of Fe-3/CN and CN.

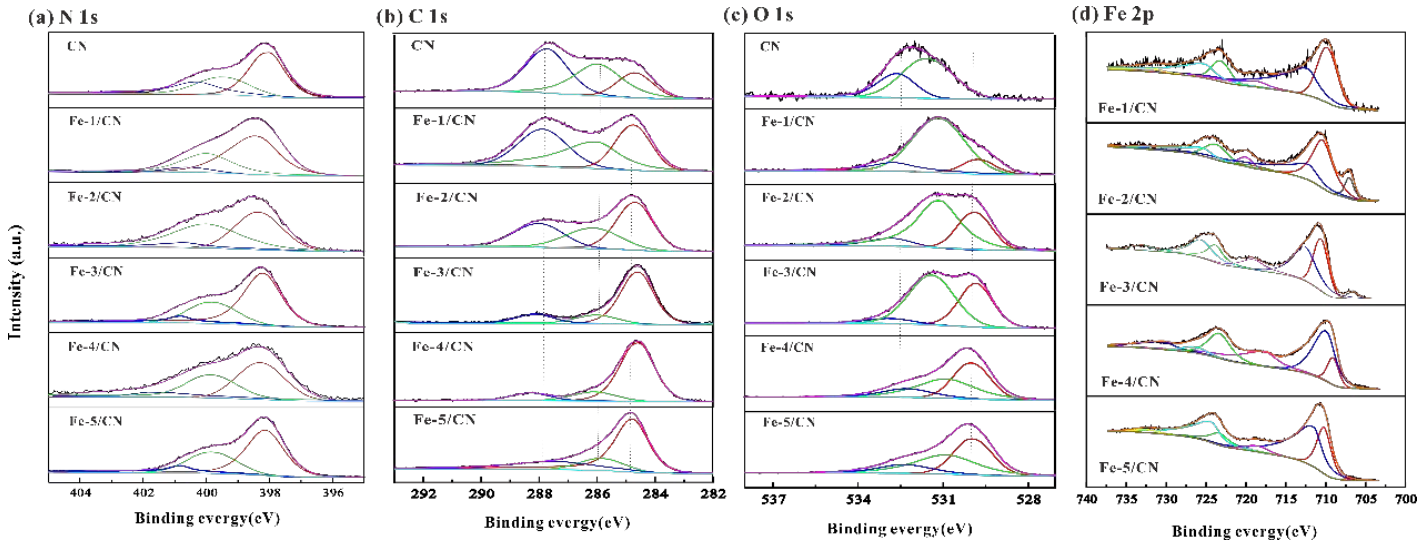

Fig. S5. N 1s (a), C 1s (b), O 1s (c), and Fe 2p (d) peaks of Fe-X/CN (X=1, 2, 3, 4, and 5).

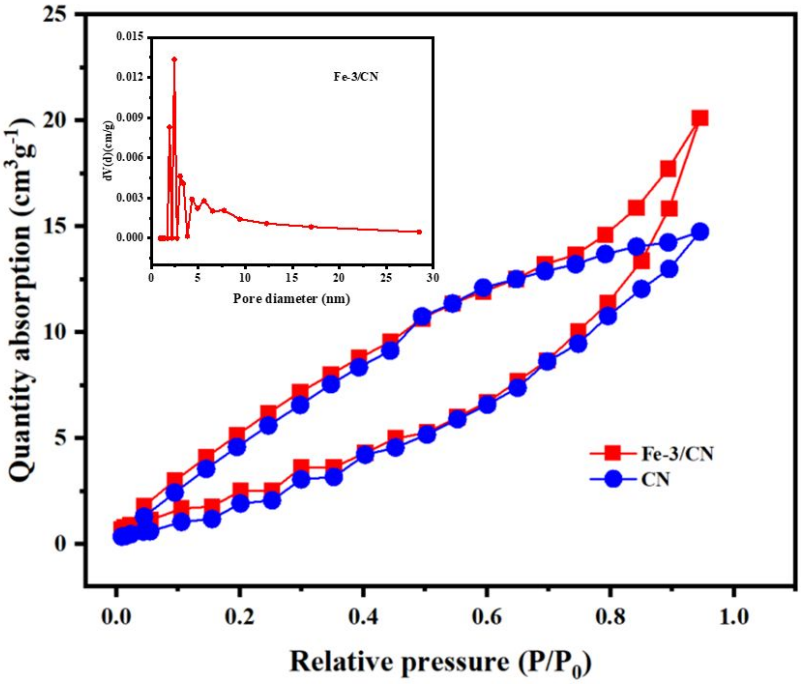

Fig. S6. Nitrogen adsorption–desorption isotherms and the corresponding pore size distributions curve (inset) of Fe-3/CN and CN.

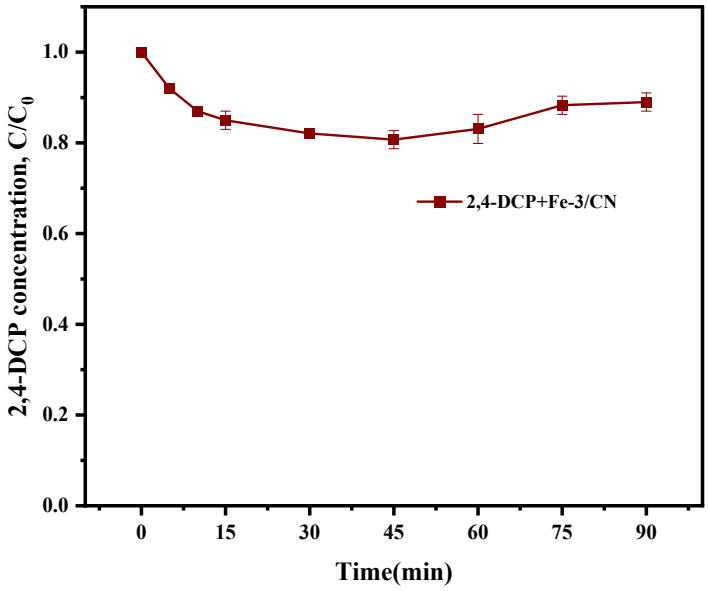

Fig. S7. 2,4-DCP adsorption - desorption equilibrium diagram.

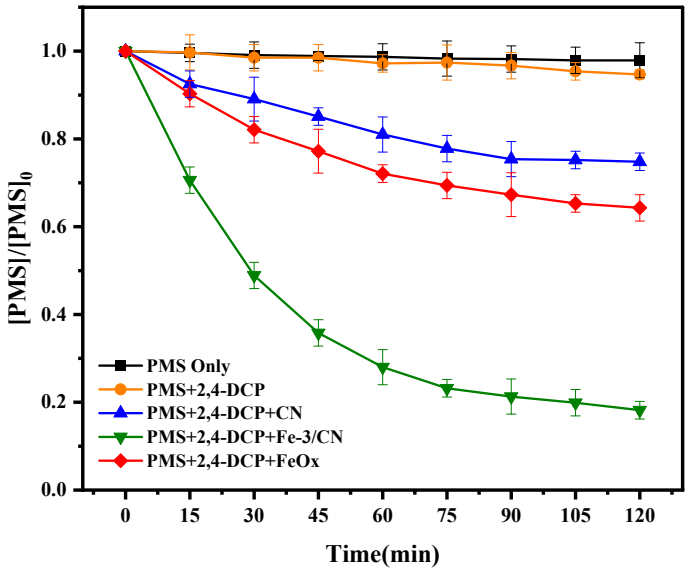

Fig.S8. Consumption of PMS under different systems. Conditions : [2,4-DCP]0 = 5 mg/L, [PMS]0 = 1.0 mM, [Catalyst]0 = 0.5 g/L, T = 298 K.

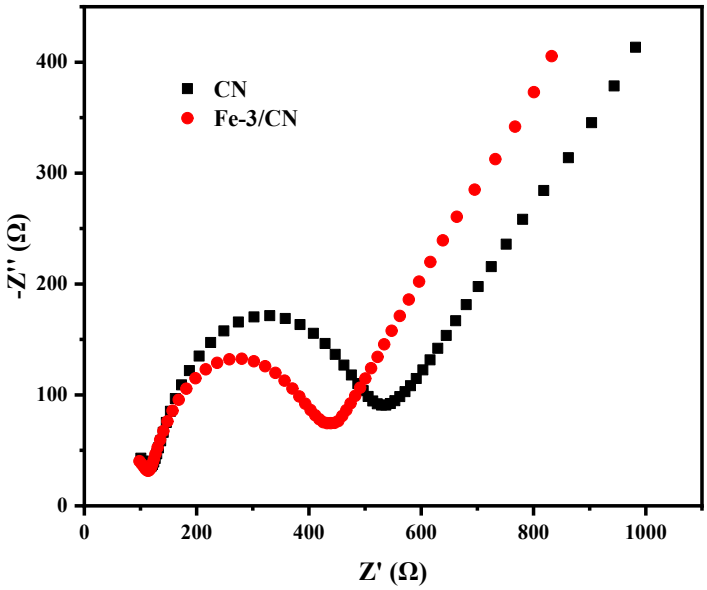

Fig. S9. The electrochemical impedance spectra of CN and Fe-3/CN.

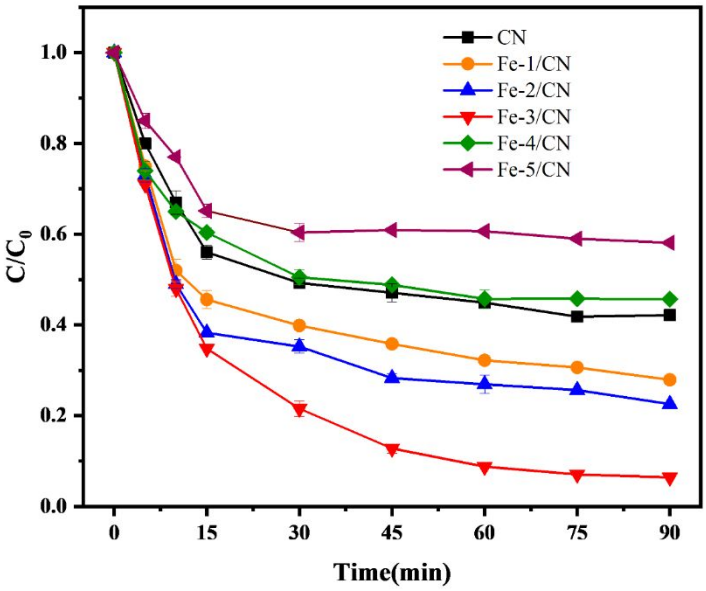

Fig. S10. Effect of Fe dosage on 2,4-DCP removal.

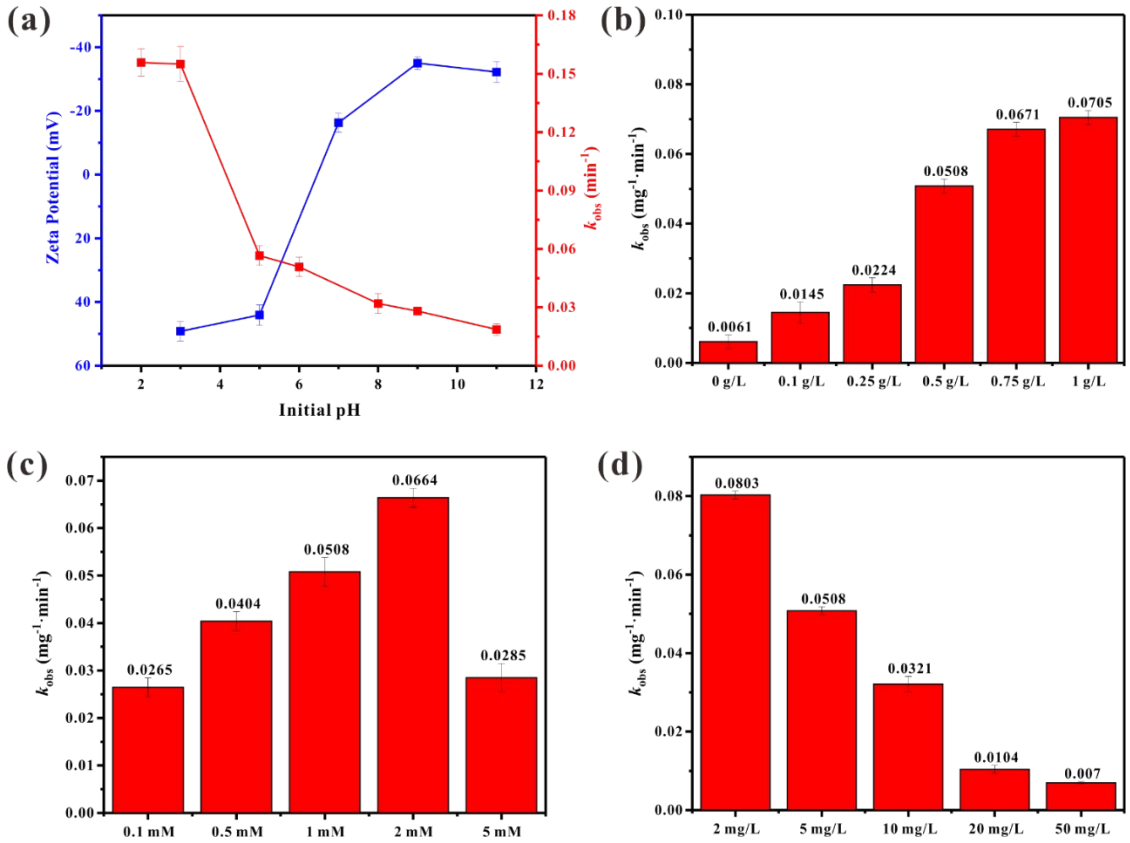

Fig. S11. The corresponding zeta potentials (blue line) and k values (red line) at different pH (a); The corresponding values of k for different factors, Fe-3/CN dosage(b), PMS concentration (c), and 2,4-DCP concentration(d).

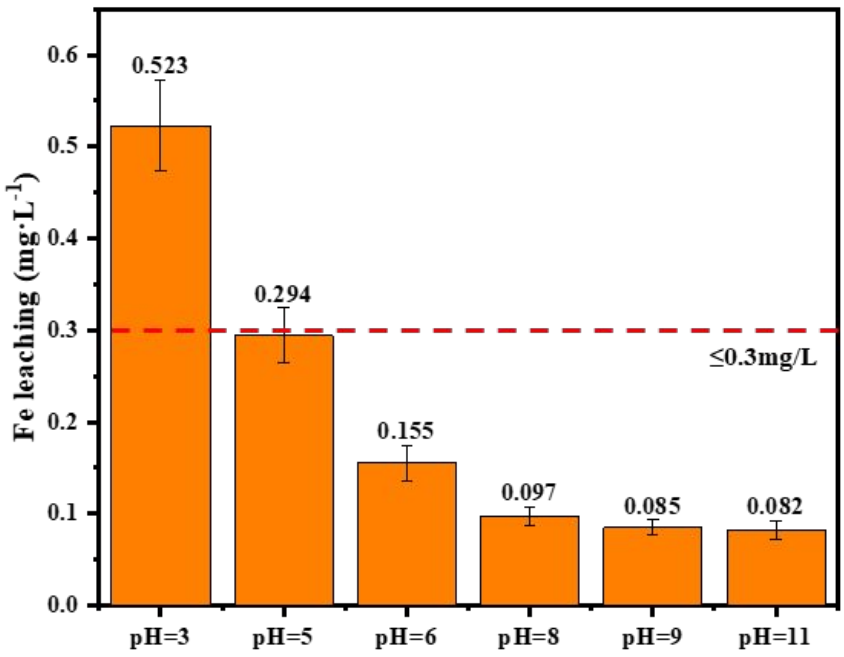

Fig. S12. The concentration of Fe leaching at different pH values.

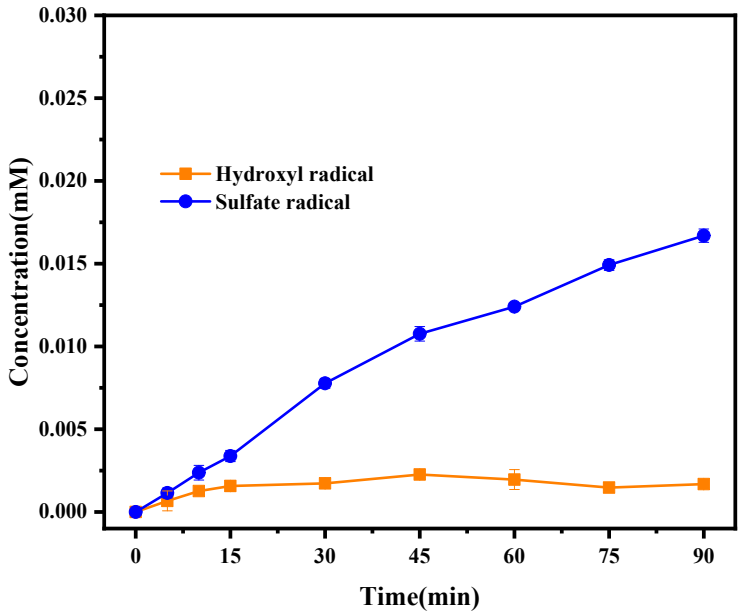

Fig. S13. Relative concentration of sulfate radical and hydroxyl radical in FeO_x/CN/PMS system.

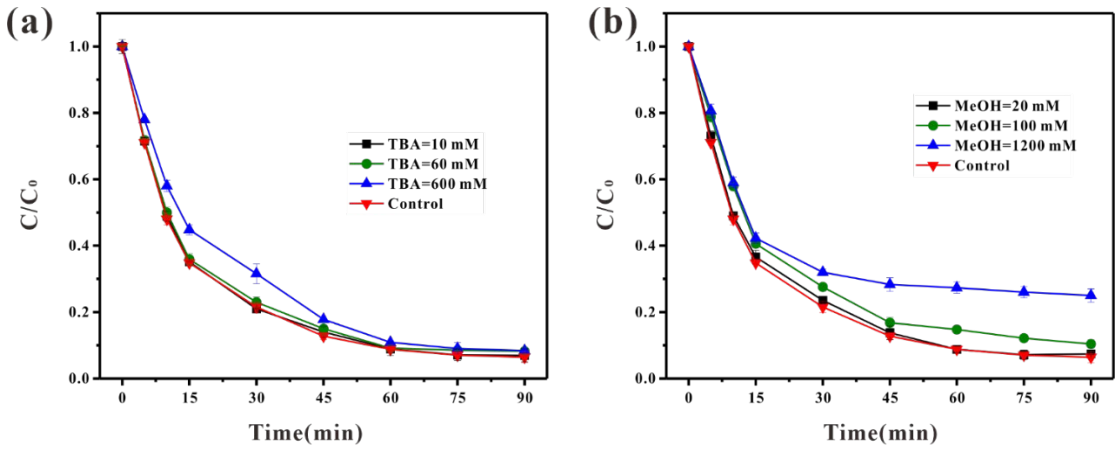

Fig. S14. Effect of different doses of TBA(a) and MeOH(b) on 2,4-DCP degradation.

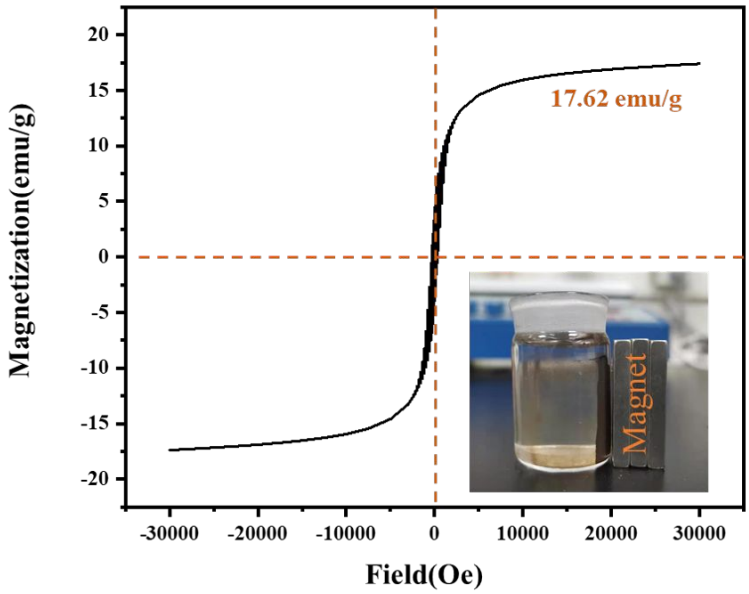

Fig. S15. Magnetization curves of Fe-3/CN.

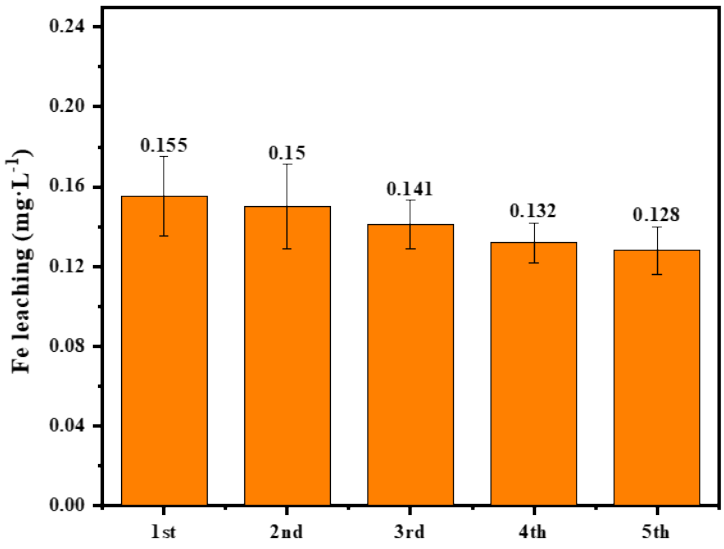

Fig. S16. The concentration of Fe leaching for each cycle.

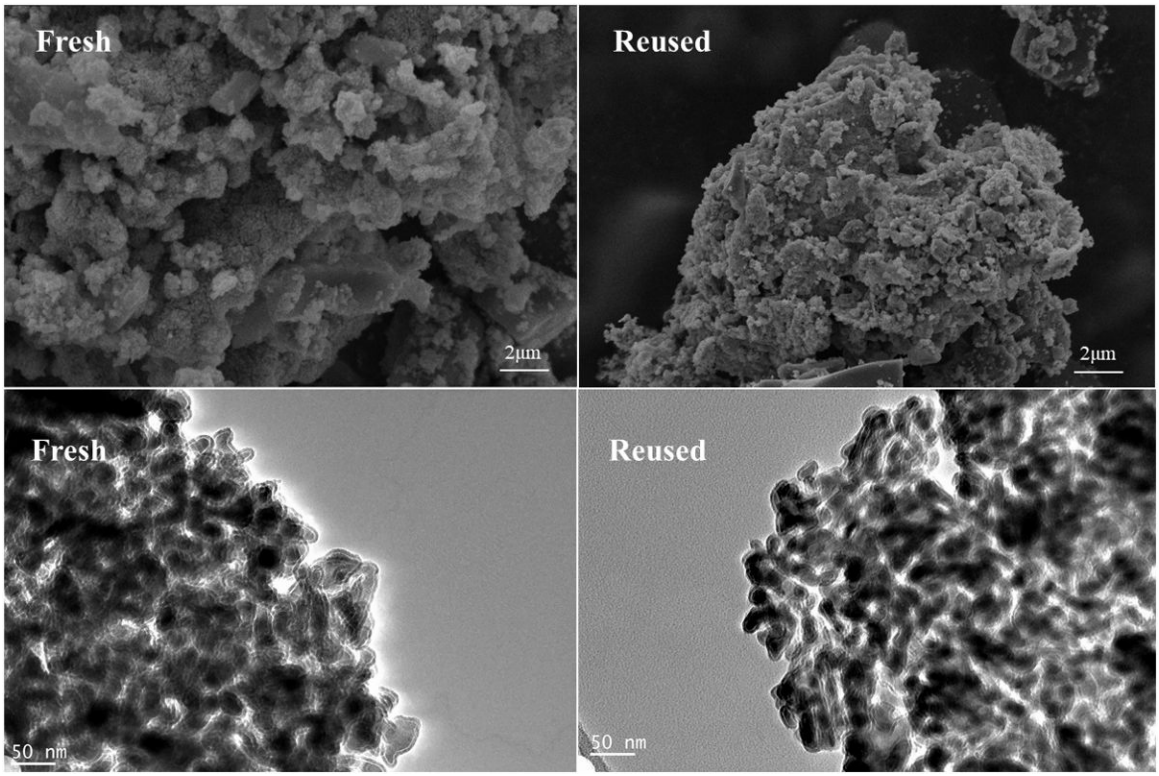

Fig. S17. SEM and TEM images of fresh Fe-3/CN and the reused.

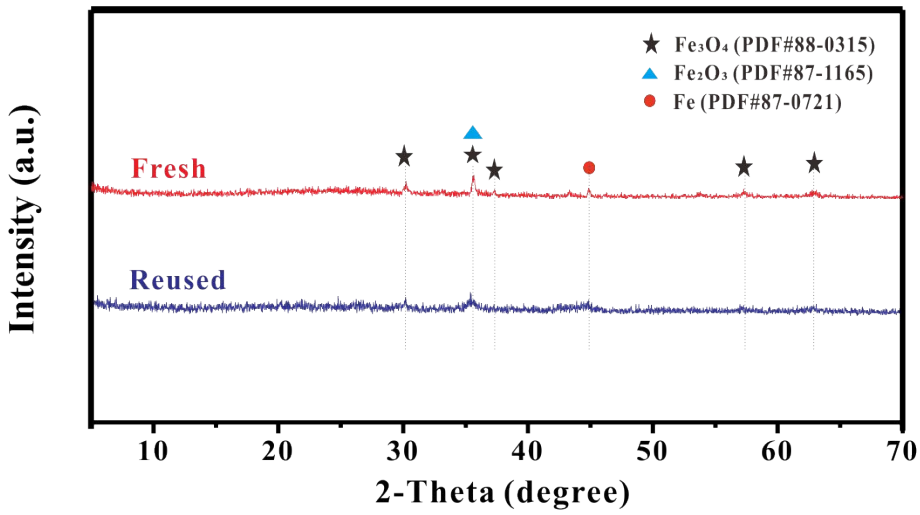

Fig. S18. The XRD spectrum of Fe-3/CN and the reused.

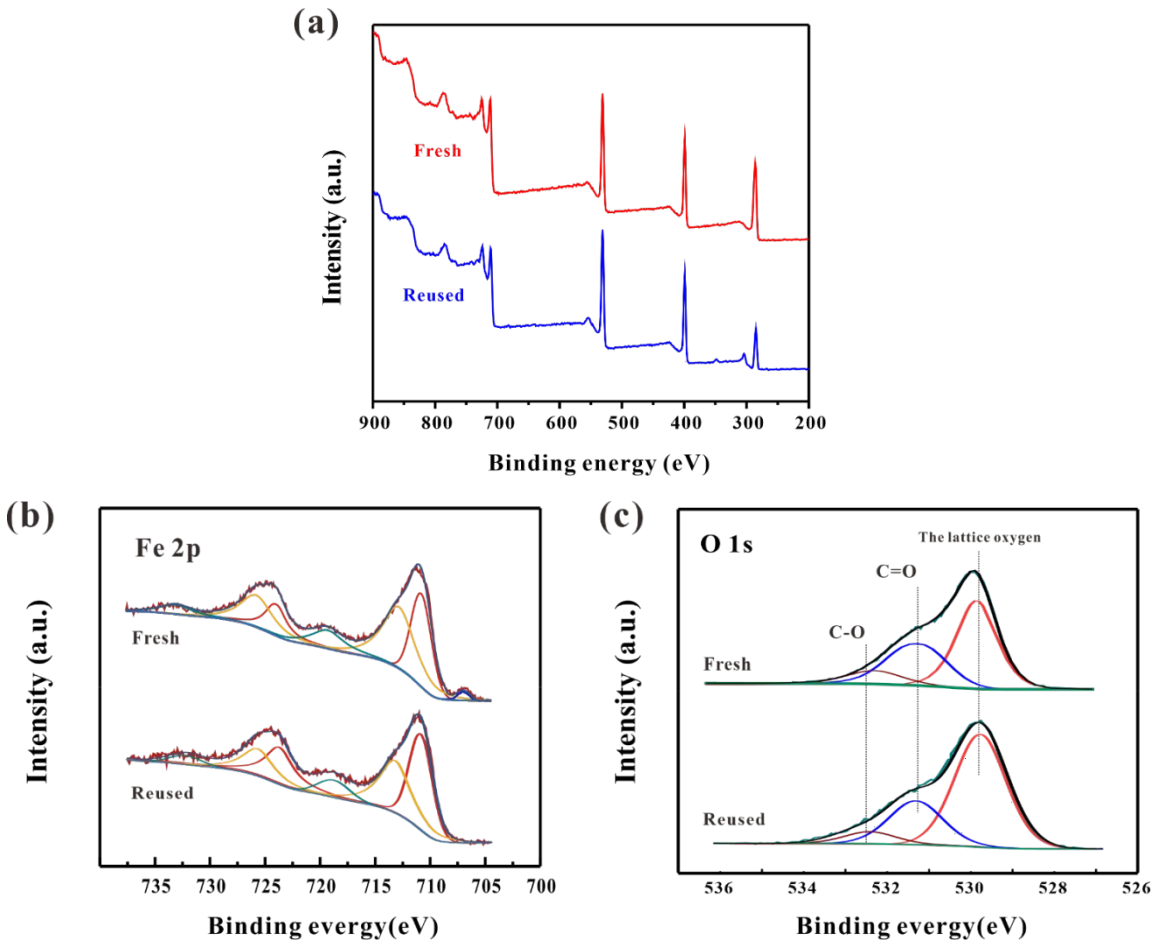

Fig. S19. XPS survey spectra of Fe-3/CN and the reused(a); Fe 2p peaks of fresh Fe-3/CN and the reused(b); O 1s peaks of Fe-3/CN and the reused(c).

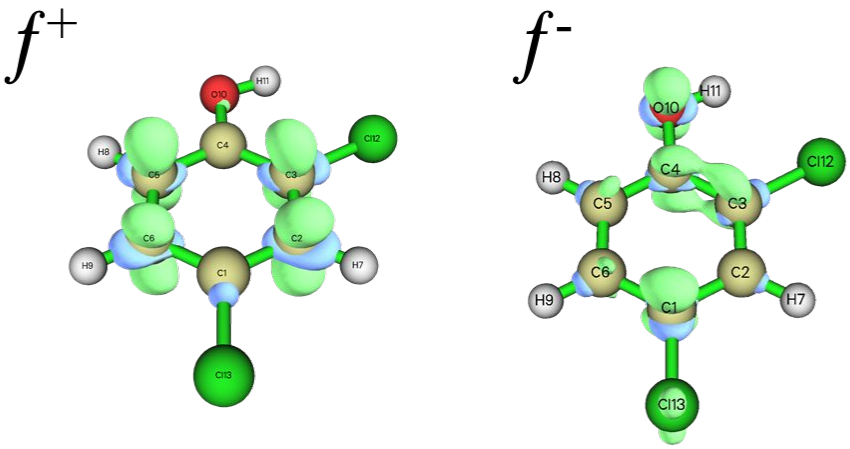

Fig. S20. The Fukui function isosurface.

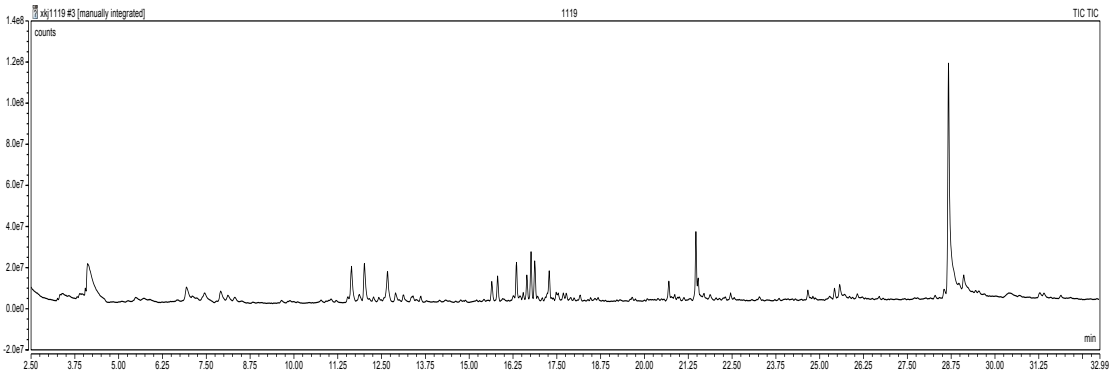

Fig. S21. GC–MS spectroscopy of the main component of the 2,4-DCP of degraded products (TIC).

Fig.S22-30. The mass spectrogram of intermediate of the 2,4-DCP degradation.

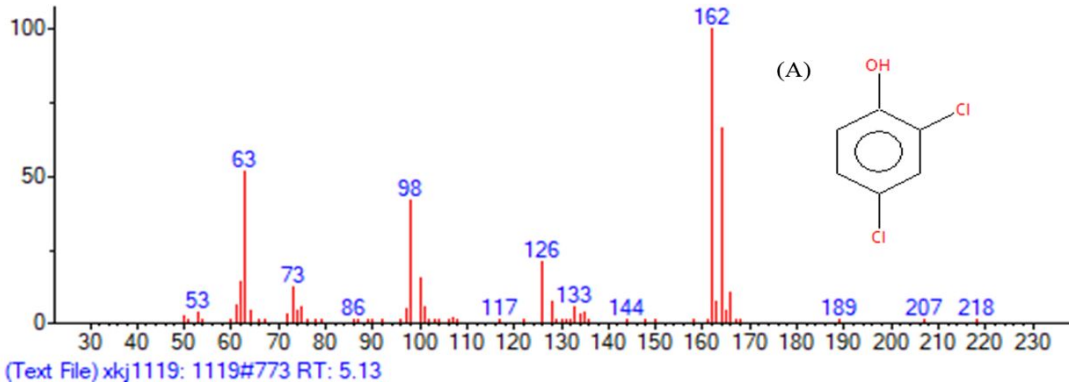

Fig. S22.

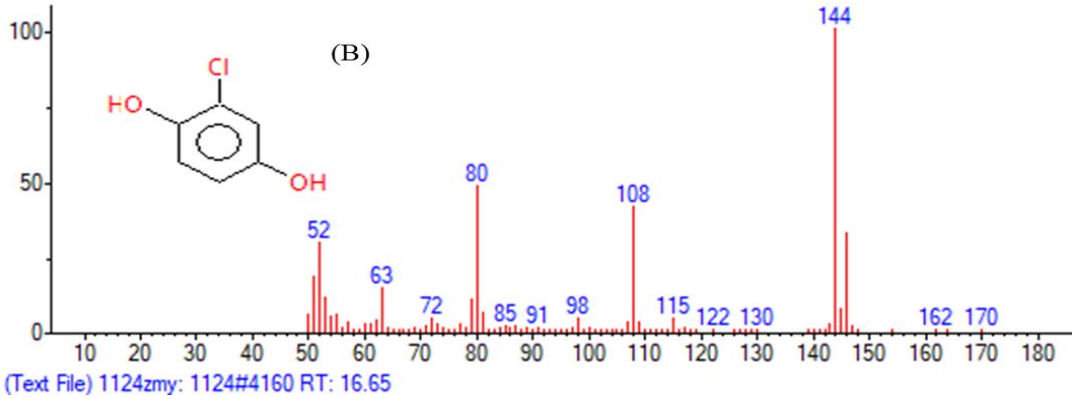

Fig. S23.

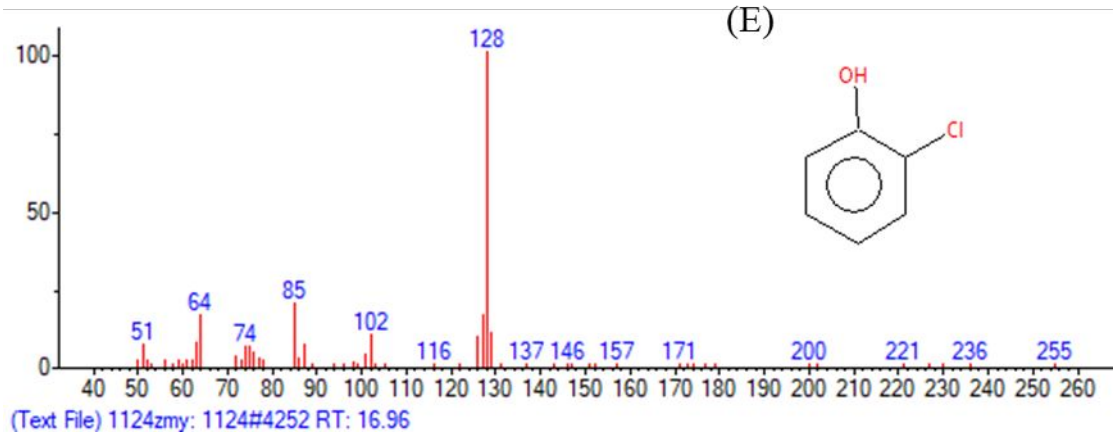

Fig. S24.

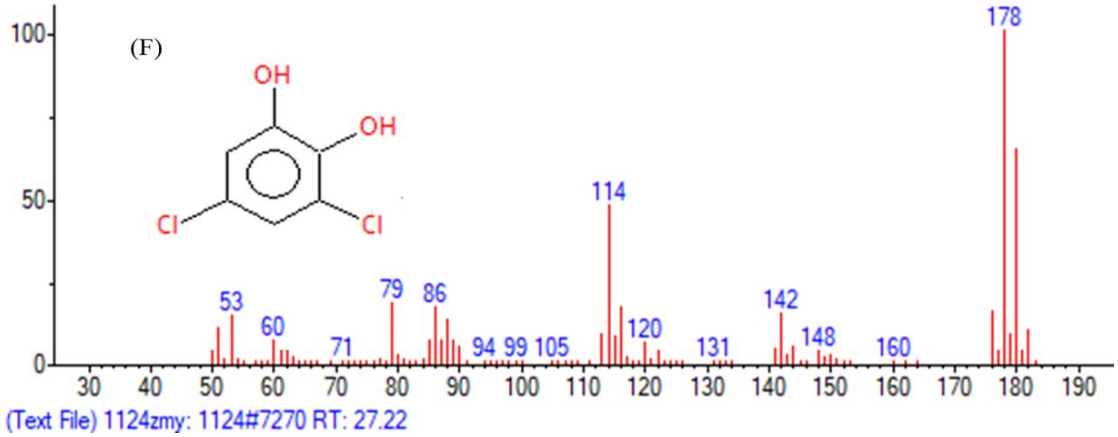

Fig. S25.

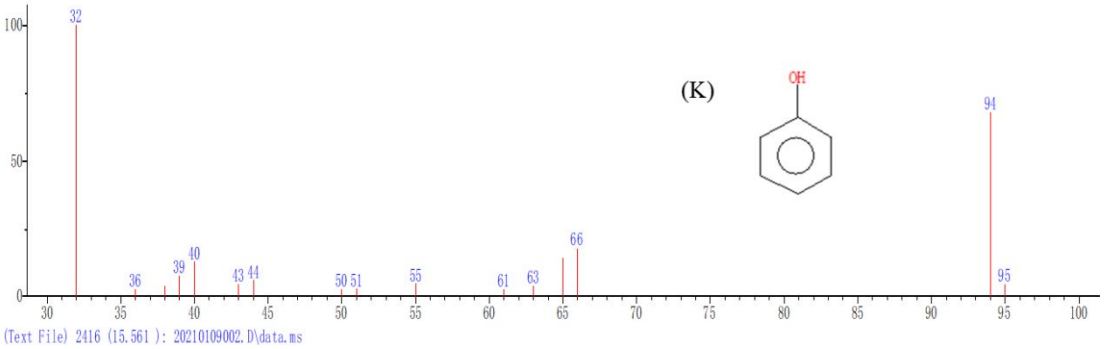

Fig. S26.

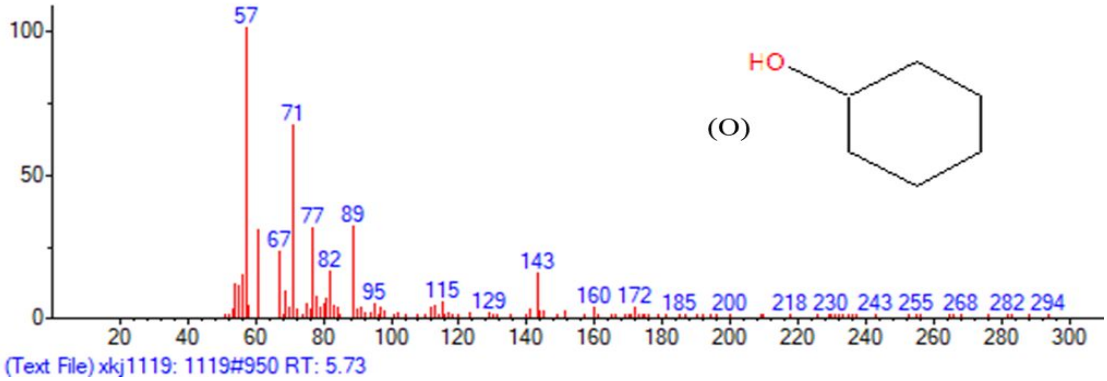

Fig. S27.

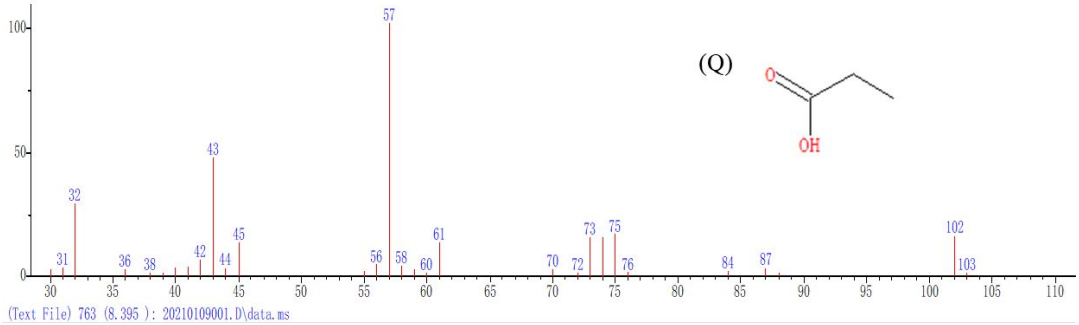

Fig. S28.

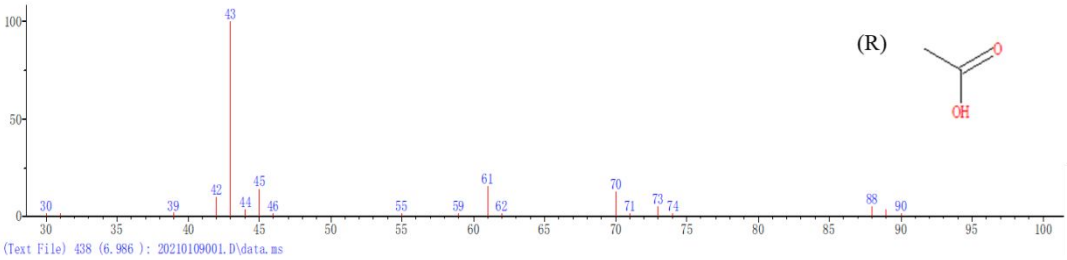

Fig. S29.

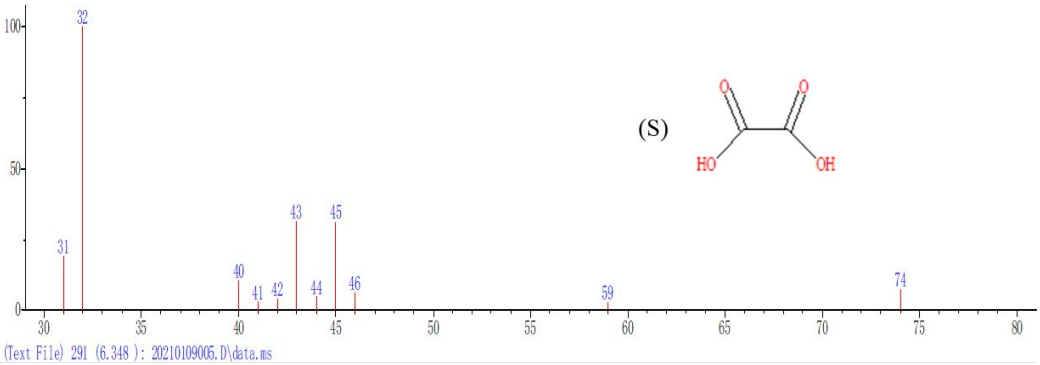

Fig. S30.

References

[1] W.D. Oh, Z. Dong, G. Ronn, T.T. Lim, Surface–active bismuth ferrite as superior peroxymonosulfate activator for aqueous sulfamethoxazole removal: Performance, mechanism and quantification of sulfate radical, Journal of Hazardous Materials (2016) 71-81. https://doi.org/10.1016/j.jhazmat.2016.11.056.

[2] M.E. Lindsey, M.A. Tarr, Quantitation of hydroxyl radical during fenton oxidation following a single addition of iron and peroxide, Chemosphere 41(3) (2000) 409-17. https://doi.org/10.1016/s0045-6535(99)00296-9.